South African Journal of Chemical Engineering 40 (2022) 48–56

Contents lists available at ScienceDirect

South African Journal of Chemical Engineering

journal homepage: www.elsevier.com/locate/sajce

Numerical solution of 3D rotating nanofluid flow subject to Darcy-Forchheimer law, bio-convection and activation energy

Muhammad Tayyab [a], Imran Siddique [b,*], Fahd Jarad [c,d,*], Muhammad Kamran Ashraf [a], Bagh Ali [e]

[a] Department of Mathematics, National College of Business Administration & Economics, Lahore, 54660 Pakistan
[b] Department of Mathematics, University of Management and Technology, Lahore, 54782, Pakistan
[c] Department of Mathematics, Cankaya University, Etimesgut, Ankara, Turkey
[d] Department of Medical Research, China Medical University Hospital, China Medical University, Taichung, Taiwan
[e] Department of Applied Mathematics, Northwestern Polytechnical University, 127 West Youyi Road, Xian, 710072, China

ARTICLE INFO

Keywords:
Darcy-Forchheimer
Bioconvection
3D Rotating Flow
Nanofluid
Activation Energy

ABSTRACT

This work discourses the dynamics of three dimensional rotating nanofluid flows subject to magnetohydrodynamic, Darcy-Forchheimer law, bioconvection self-motive microorganism, and activation energy. The numerical procedure is indicated when close agreement of the current finding is attained in comparison with the existing ones as limiting case. The leading equations based on preservation of mass, momentum, and energy are formulated with partial derivatives which are then transmuted into dimensionless differential form with the enactment of apposite similarity transformations. So, to tackle the non-linearity of these equations, numerical procedure based on shooting technique and Runge-Kutta method is bound to be coded on MATLAB platform. The emerging parameters are varied to observe the change of microorganism distribution, velocity, concentration of nano species, and temperature distribution. Results are displayed graphically and discussed. It is noticed that liquid velocity is decelerated against the constraints of inertia and porosity. The temperature field is strengthened with thermophoresis and Brownian motion. The concentrations of nanoparticle and microorganism are depreciated against Lewis number and bio-Lewis number respectively. The concentration of microorganism is improved for greater peclet number Pe but it lessens with growth in bioconvection Lewis numberL_b. The function $\theta(\eta)$ and $\varphi(\eta)$ showed increasing response to thermophoresis parameter N_t. The parameter of Brownian motion has noticeable growing impact on concentration of nano particles but decreasing N_b for $\theta(\eta)$ temperature.

1. Introduction

The fluids which have nanometer sized particles of matter are called nano-fluids. Nano fluids are actually composed by colloidal interruption of nanoparticles in given base liquid. Initially Choi and Eastman (Choi and Eastman, 1995) gave the idea of mixing of nano sized particles in the base fluid. Mostly the nano fluids have nano-particles such as carbon nano tubes, metals, carbides, and oxides. Widely used base fluids are oils, ethylene glycol and water. Recently, many experts (Kasaragadda et al., 2020, Kumar et al., 2021, Khan et al., 2014, Ali et al., 2020, Hayat et al., 2016) have engrossed to explore the nanotechnology due to its vast application in industrial process including pharmaceutical processes, microelectronics, cooling in vehicle engine, heat exchanger, washing machines, and advanced nano-technological products. Buongiorno (Buongiorno, 2006) offer the concept of Brownian motion effect, unusual two slip phenomena and thermophoresis for enhancement of heat transportation. Mass and heat transfer analysis with unsteady magneto-hydrodynamic flow of hybrid nanofluid elaborated by Sreedevi et al. (Sreedevi et al., 2020). The analysis of dynamic of micropolar conveying tiny particles of nano-sized subject to porous media considered by Kishan and Deepa (Kishan and Deepa, 2012). The significance of Joule heating on nanofluid pass over a vertical surface measured by Alim et al. (Alim et al., 2008). Hayat et al. (Hayat et al., 2020) Analyzed Darcy -Forchheimer flow to the curved extending surface in the existence of partial slip. The boundary-layer nanofluid flow passing over a stretching sheet was elaborated by Khan et al. (Khan and Pop, 2010).

The flow of fluid is known as rotating flow, if the twist of the fluid's

* Corresponding author.
E-mail address: imransmsrazi@gmail.com (I. Siddique).

https://doi.org/10.1016/j.sajce.2022.01.005
Received 22 November 2021; Received in revised form 4 January 2022; Accepted 18 January 2022
Available online 20 January 2022

velocity is not zero. In recent decays, the study of heat transfer problems subject to rotating frame of reference is purely interested matter, which is the consequence of their wide usage in the department of assembling of crystal, thermal power station, rotating machines, food handling, computer stockpiling devices, and gas turbine rotators. First of all, Wang (Wang et al., 2020) was introduced the principal endeavor towards rotating flow. Kotresh et al. (Kotresh et al., 2021) introduced the computational analysis of rotating nano fluid flow past a stretched surface. Krishna et al. (Krishna and Chamkha, 2020) looked on MHD elastic-viscous fluid's flow in the existence of Hall and slip effects in the rotating medium.

Bioconvection is a fact that to specify the unstructured plan and instability action by the microorganism, which are swimming to the upper part of a fluid, has a lesser density. Therefore, its upward migration will produce a combination of asymmetric mass transfer and surface instability throughout the fluid. In recent, the concept of relativity of bio-convection with low concentration has a vital role in a suspension of nano particles for scholars. Bioconvection helps to rise the rate of mass transportation. Mondal and Pal (Kanta Mondal and Pal, 2020) Studied the generation of entropy in bio-convection flow of nano liquid amongst two extendable rotating disks. Sk et al. (Sk et al., 2016) examined multiple slip impacts on bio-convective channel of MHD nanofluid flow due to microorganisms. Kuznetsov and Avramenko (Kuznetsov and Avramenko, 2004) elaborated stability of gyrotactic micro-organism suspension through bioconvective flow. Many authors contributed in this field (Zeeshan et al., 2020, Makinde and Animasaun, 2016, Makinde and Animasaun, 2016, Avinash et al., 2017) due to its vast applications in various chemical processes to enhance the heat transfer rate. Thermobioconvective flow of tangent hyperbolic nanofluid over an extending surface was examined by Shafiq et al. (Shafiq et al., 2020, Shafiq et al., 2021)

An atomic system obtain energy before a process (such as reaction or emission) is known as activation energy. In various processes: like heat transfer, geothermal, catalytic, atomic reactors and geophysics, there is the inclusion of convection flow in view of a porous medium. Permeable porous space is very powerful in groundwater frameworks, energy stockpiling units, the movement of water in supplies, solar receiver, and so on. Ali et al. (Ali et al., 2020) explored MHD stream of time dependent Maxwell nano fluid through rotating stretched surface in existence of activation energy and double diffusion. Encouragement of bioconvective Maxwell nanofluid with impact of thermophoresis and Brownian motion past a Riga plate inspected by Ali et al. (Ali et al., 2021). Gowda et al. (Gowda et al., 2021) investigated the two-dimensional flow of incompressible nanofluid and rate of reaction for the activation energy parameter. The bioconvective flow and heat transfer in a porous cavity with chemical reaction and activation energy studied by Balla et al. (Balla et al., 2020). Many authors have contributed their efforts in the study of hybrid nanofluid flow with Arrhenius activation energy (Varun Kumar et al., 2021, Ramesh et al., 2021, Shi et al., 2021, Madhukesh et al., 2021)

A comprehensive survey of existing literature convinces that nano fluid bioconvection of rotational flow due to an extending surface is rarely conferred. Sadia et al. (Rashid et al., 2018) intended the activation energy of 3-dimensional Darcy-Forchheimer rotating flow. Here the limitation pertains to lesser heat conduction ability of the base fluid and hence inefficient thermal transportation is resulted. The major motivation of this work is to incorporate nano particle inclusion to enhance the thermal conductivity and to make efficient heat transport. However, to sidestep the probable settling of nano objects, bioconvection of microorganisms is opted as novel aspect of this work. Also the model is developed for the evaluation of the behavior of Brownian Motion and thermophoresis. The findings obtained here in are expected to be utilized for better thermal efficiency of heat exchangers to maintain thermal balance management in the compacts heat density equipment's and gadgets.

2. Physical model

With the consideration of the following assumptions that fluid is incompressible. The flow of fluid is three dimensional and is supposed to be steady. The electrically conducting fluid is viscous in form. Radiation and dissipation effects are ignored. The flow is over a porous space which accords with the plane z=0 and the flow is limited in the section z>0. Two balance forces used along the *x*-axis in opposite direction to maintain the sheet extended and possessed the origin fixed. The z-axis taken along and perpendicular to the sheet. All the characteristic are considered constant around the motion in the fluid. Nanofluid is characterized with thermophoresis and Brownian movement. The motile microorganism's density n.

The governing equations of motion are given below: (Buongiorno, 2006, Rashid et al., 2018, Kuznetsov, 2011)

$$\frac{\partial u}{\partial x}+\frac{\partial w}{\partial z}+\frac{\partial v}{\partial y}=0 \tag{1}$$

$$\frac{\partial u}{\partial x}u+\frac{v}{K}u+\frac{\partial u}{\partial y}v+\frac{\partial u}{\partial z}w-2\Omega v=\frac{\partial^2 u}{\partial z^2}v-Fu^2 \tag{2}$$

$$\frac{\partial v}{\partial x}u+\frac{v}{K}v+\frac{\partial v}{\partial y}v+\frac{\partial v}{\partial z}w+2\Omega u=\frac{\partial^2 v}{\partial z^2}v-Fv^2 \tag{3}$$

$$u\frac{\partial T}{\partial x}-\alpha\frac{\partial^2 T}{\partial z^2}+\frac{\partial T}{\partial y}v+\frac{\partial T}{\partial z}w=T^*\left[\frac{\partial T}{\partial z}\frac{\partial C}{\partial z}D_B+\left(\frac{\partial T}{\partial z}\right)^2\frac{D_T}{T_\infty}\right] \tag{4}$$

$$u\frac{\partial C}{\partial x}-k_r{}^2(C_\infty-C)\left(\frac{T}{T_\infty}\right)e^{-\frac{Ea}{kT}}+v\frac{\partial C}{\partial y}+w\frac{\partial C}{\partial z}=DC\nabla^2+\frac{\partial^2 T}{\partial z^2}\frac{D_T}{T_\infty} \tag{5}$$

$$\frac{\partial n(u)}{\partial x}+\frac{\partial n(v)}{\partial y}+\frac{\partial n(w)}{\partial z}+w_c\frac{b}{(C_w-C_\infty)}\left[\frac{\partial}{\partial z}\left(\frac{\partial C}{\partial z}n\right)\right]=D_m\frac{\partial^2 n}{\partial z^2} \tag{6}$$

Here u, v and w are the velocity components and υ is kinematic viscosity, ρ used for the density, κ indicates the vortex density, μ is used for viscosity coefficient, σ is the constant of electrical conduction of the liquid, T is used for temperature of fluid,T_∞ mention for ambient temperature, K mention for heat conductivity of liquid, c_p mention for the heat capacity. Here $(\nu=\mu/\rho)$represents kinematics viscosity, K permeability of porous, $c_b$the drag coefficient, u dynamics viscosity, mediumF $=C_b/xk^{1/2}$ non uniform coefficient of inertia (Ali et al., 2021, Zhao et al., 2010), α heat diffusibility of liquid.

The boundary conditions are: (Rashid et al., 2018)

$$v\to 0,\ u\to 0,\ C\to C_\infty,\ n\to n_\infty,\ T\to T_\infty \text{ when } z\to\infty \tag{7}$$

Where T_w denotes the wall temperature, C_∞ is the concentration beyond the wall and extending rate $(a>0)$. Using similarity transformations: (Ali et al., 2020)

$$\eta=\sqrt{\frac{a}{\nu}}z,\ v=axg(\eta),\ u=axf'(\eta),\ w=-f(\eta)(av)^{1/2} \tag{8}$$

$$\theta(\eta)(T_w-T_\infty)=(T-T_\infty),\ \varphi(\eta)=\frac{C-C_\infty}{C_w-C_\infty},\ (n_w-n_\infty)\chi(\eta)=(n-n_\infty)$$

Equation (5) is verified while equation (2)-(6) become;

$$f'''-\lambda f'+ff''+2\beta g-f'^2(1+F_r)=0 \tag{9}$$

$$g''-f'g+fg'-\lambda g-2\beta f'-F_rg^2=0 \tag{10}$$

$$\theta''+\left(N_b\theta'\varphi'+f\theta'+N_t\theta'^2\right)Pr=0 \tag{11}$$

$$\frac{1}{Sc}\varphi''+f\varphi'+\frac{1}{Sc}\frac{N_t}{N_b}\theta''-\sigma[1+\delta\theta]^n\exp\left[-\frac{E}{1+\delta\theta}\right]\varphi=0 \tag{12}$$

$$\chi'' + L_b f\chi' - Pe(\varphi''(\chi+\delta_1)+\chi'\varphi') = 0 \quad (13)$$

With reduced conditions:

$$f' = 0,\ f = 0,\ \theta = \varphi = 1\ g = 0,\ at\ \chi = 1,\ \eta = 0,$$

$$g\to 0,\ f'\to 0,\ \varphi\to 0,\ \theta\to 0,\ \chi\to 0,\ at\ \eta\to\infty \quad (14)$$

Note that $\lambda = \frac{v}{ka}$ represents porosity parameter, $\beta = \frac{\Omega}{a}$ is rotational parameter, $F_r = \frac{C_b}{k^{\frac{1}{2}}}$ inertia coefficient, $\Pr = \frac{v}{\alpha}$ the prandtl number, $\sigma = \frac{k^2}{a}$ reaction rate, $Sc = \frac{v}{D}$the Schmidt number, $L_b = \frac{v}{D_m}$ The Lewis number,$Pe = \frac{bw_m}{D_m}$ the peclet number$N_b = \frac{T^* D_B}{v}$ Brownian motion and$N_t = \frac{T^* D_T}{vT_\infty}$thermophoresis.

Skin friction coefficient, Sherwood number, and Nusselt number are:

$$Nu_x = \frac{xq_w}{k(T_w - T_\infty)},\ Sh_x = \frac{xj_w}{D(C_w - C_\infty)},\ N_x = \frac{xk_w}{D_m(n_w - n_\infty)}, \quad (15)$$

$$C_f = \frac{T_w}{\rho {U_w}^2},\ T_w = \mu\left(\frac{\partial u}{\partial z}\right)$$

With:

$$q_w = -k\frac{\partial T}{\partial z}|_z,\ j_w = -\left(\frac{\partial C}{\partial z}\right)D|_z = 0,\ k_w = -\left(\frac{\partial n}{\partial z}\right)D_m|_z = 0 \quad (16)$$

Here, we have:

$$C_f\sqrt{\mathrm{Re}_x} = f''(0),\ \frac{Nu_x}{\sqrt{\mathrm{Re}_x}} = -\theta'(0),\ \frac{Sh_x}{\sqrt{\mathrm{Re}_x}} = -\varphi'(0),\ \frac{N_x}{\sqrt{\mathrm{Re}_x}} = -\chi'(0) \quad (17)$$

In which $\mathrm{Re}_x = \frac{ax^2}{v}$ shows local Reynolds number.

3. Numerical approach

The resulting boundary value problem consisting of equation (9) to (14) involve non-linear terms which make it hard to yield analytical solution. A numerical approach based on Runge-Kutta method and shooting is hired to attain viable solution. In order to implement the scheme, an equivalent first order system of equations is obtained as given below:

$$(f_1, f_4, f_6, f_8, f_{10}) = (f,\ g,\ \theta,\ \varphi,\ \chi)$$

$$f_1' = f_2$$

$$f_2' = f_3$$

$$f_4' = f_5$$

$$f_6' = f_7$$

$$f_8' = f_9$$

$$f_{10}' = f_{11}$$

$$f_3' = -f_1 f_3 + \lambda f_2 - 2\beta f_4 + (1+F_r){f_2}^2$$

$$f_5' = -f_1 f_5 + f_2 f_4 + 2\beta f_2 + \lambda f_4 + F_r {f_4}^2$$

$$f_7' = -\Pr\left(f_1 f_7 + N_b f_7 f_9 + N_t f_7^2\right)$$

$$f_9' = Sc[\sigma(1+\delta f_6]^n \exp\left[-\frac{E}{1+\delta f_6}\right] f_8 - \frac{N_t}{N_b} f_7' - Sc f_1 f_9$$

$$f_{11}' = P_e(f'_9(f_{10}+\delta_1)+f_{11}f_9) - L_b f_1 f_{11}$$

The boundary conditions are:

Table 1
Numerical results for $-f''(0)$ and for numerous values of β, λ, Fr

β	λ	Fr	Sadia et al. (Rashid et al., 2018)	Present outcomes
1	0.2	1	1.58724	1.587236
2			1.862267	1.862673
3			2.10932	2.109315
0.5	0.1		1.41806	1.4180632
	0.5		1.53031	1.530305
	1		1.67153	1.671530
	0.2	1	1.36352	1.363524
		2	1.58502	1.585020
		4	1.96195	1.961949

Table 2
Numerical results for $-\theta'(0)$ and for numerous values of λ, β, Pr, Fr

λ	β	Pr	Fr	**Sadia et al.** (Rashid et al., 2018)	**Present outcomes**
0	0.5	1	1	0.508972	0.5089724
1				0.485852	0.4858519
2				0.457520	0.4575203
0.2	0.1			0.542198	0.5421983
	0.5			0.506965	0.5069652
	0.9			0.467794	0.4677941
	0.5	2		0.811336	0.8113356
		3		1.064611	1.0646115
		4		1.278977	1.2789778
		1	0	0.844615	0.8446151
			2	0.783173	0.7831728
			3	0.734272	0.7580794

Table 3
Results for, $-\theta'(0)$ for various values of λ, β, Fr, N_t, N_b

λ	β	**Nt**	***Fr***	***Nb***	$-\theta'(0)$
0	0.5	0.1	1	0.1	0.9055
1					0.8639
2					0.8186
0.2	0.1				0.9286
	0.5				0.8988
	0.9				0.8533
	0.5	0.1			0.8988
		0.2			0.8396
		0.3			0.7842
		0.1	0		0.9303
			2		0.8717
			3		0.8473
			1	0.4	0.6408
				0.5	0.5668
				0.6	0.4988

$$f_2 = 0,\ f_1 = 0,\ f_6 = f_8 = 1\ f_4 = 0,\ at\ f_{10} = 1,\ \eta = 0,$$

$$f_4\to 0,\ f_2\to 0,\ f_8\to 0,\ f_6\to 0,\ f_{10}\to 0,\ \text{at}\ \eta\to\infty.$$

4. Discussion

Numerical evaluation has been measured for different amount of the parameters namely λ, β, *Fr, Pr, E*, N_b, N_t. The impacts of these parameters have been studied on temperature, skin friction co-efficient, microorganisms and heat transfer distributions, velocity and Nusselt number. Physical parameters involved in present investigation have fixed values such as: $P_r = 1.0,\ Nt = 0.1,\ E = F_r = 1.0,\ N_b P_e = 0.1,\ m = L_b = 1.0,\ \beta = 0.5,\ \lambda = 0.2,\ L_e = 1.0,\ \sigma = 0.6,\ S_c = 0.25$.Table 1 to Table 4 contain the results for $-f''(0)$, $-\theta'(0)$ and for bioconvection $-\chi(0)$.

An assessment of the present arithmetical results with the previous results are presented in these tables. The comparison is excellent. Also, the Table 1 represents a comparison of the results of $-f''(0)$ for fluids under the influence of parameter β. The skin friction number gets

Table 4
Results for $-\chi'(0)$ and for various values of λ, β, Fr, N_t

λ	β	Fr	Nt	$-\chi'(0)$
0	0.5	1	0.1	0.4847
0.5				0.4777
1.5				0.4446
0.2	0.7			0.4551
	1			0.4181
	1.5			0.3745
	0.5	2		0.4620
		3		0.4426
		4		0.4238
		1	0.1	0.4840
			0.3	0.2084
			0.5	0.0444

stronger via Fr, β and λ. This observation agrees with the previous literature. The physical reason is that, these parametrs offer resistance to fluid flow. Table 2 is prepared for$Nu_x/\sqrt{\mathrm{Re}_x}$ Nusselt number. It displays that local Nusselt number coefficient declines via rotation parameter β and porosity λ. This observation also bears a good connection with the previous results. In current investigation the ranges for the physical parameters that are involved in this work, are as follows: $0.1 \le N_b \le 1.5, 0.1 \le \lambda \le 3.0, 0.0 \le \beta \le 4.0, 0.0 \le F_r \le 7.0$, $0.0 \le P_r \le 1.2$, $0.1 \le N_t \le 0.9$, $0.0 \le E = m \le 4.0$, $0.6 \le \sigma \le 2.5$, $0.25 \le S_c \le 3.0$, $0.1 \le P_e \le 1.0$, $1.0 \le L_b \le 2.0$.

Table 3 contains the results for local Nusselt number $-\theta'(0)$ under the influence of β, Fr,N_b,N_t,λ. It is detected that magnitude of Nusselt number decreases with increase in the values of β, Fr, N_b, N_t, λ. Table 4 contains the result of bioconvection $-\chi(0)$ under the influence of β, Fr, N_t, λ. It is realized that the magnitude of $-\chi'(0)$ declines with rise in the values of β, Fr, N_t, λ.

Further this portion consist of graphical representation of physical variables$f'(\eta)$, $\theta(\eta)$, $\varphi(\eta)$and $\chi(\eta)$. Fig. 1 indicates, how parameter β effects on $f'(\eta)$. Hence an accession is observed that β causes a decline in velocity $f'(\eta)$.We noted for excessive β the elongating rate of sheet lower and so velocity depreciate. Fig. 2 depicts alteration of porosity parameter λ on velocity. The result of porosity parameter on $f'(\eta)$ interpret the same trend as that of β. Fig. 3 shows velocity for enlarging Fr. Velocity is reduced by Fr. The influence of rotation parameter on $\theta(\eta)$ with thermal layer breadth are shown in figure. Both the parameters are enlarging function of β. Fig. 5 exhibits the impact of temperature $\theta(\eta)$ on porosity parameter. It is observed that higher resistance and viscosity produces more heat and resultantly $\theta(\eta)$ increases. Fig. 6 displays the impact of temperature for values of Fr. Obviously θ is a growing function of Pr. Fig. 7 is conspired to explore Pr on$\theta(\eta)$. Physically $\theta(\eta)$ is a reducing function of Pr. Fig. 8 is sketched to explore that how temperature affect varies with Brownian motion parameterN_b. By increasing value of N_b shows temperature field also upgrade. In Fig. 9 display the effect of N_t on temperature. An expansion in N_t shows upgrade in thermophoresis. Fig. 10 reveals impact of β on concentration$\varphi(\eta)$. It is found φ is increasing for larger value of β. As we can see in Fig. 11 for porosity parameter concentration is an increasing function. In Fig. 12 we can see effects of Fr on φ. One can watch for larger value of Fr concentration distribution $\varphi(\eta)$ is increasing. Fig. 13 are sketched for larger value of Pr yields lower absorption $\varphi(\eta)$ and connected layer breadth. Fig. 14 is drawn to inspect the effects of E (activation energy). Here, we can see E maximize the concentration layer clotting. Fig. 15 and 16 illustrates for n micro-organism concentration and σ thermal diffusivity on concentration$\varphi(\eta)$. When n or σ enhance there is a rise in$\sigma[1+\delta\theta]^n \exp\left[-\frac{E}{1+\delta\theta}\right]$. It is observed that rise in the value of σ there is increment in the damaging rate of chemical reaction. Furthermore, it is dissolve or eliminate the fluid specie enhanced precisely and in result concentration

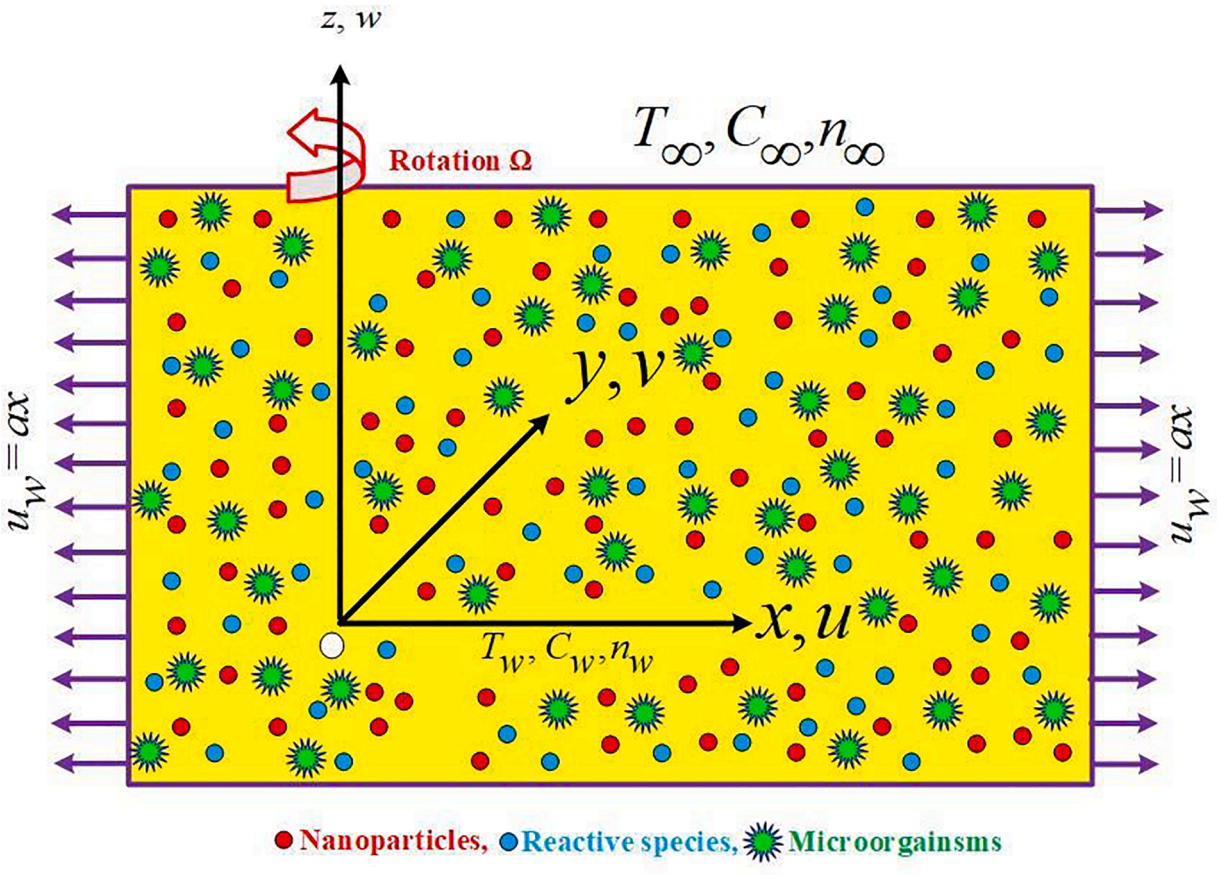

Fig. 1. Problem geometry with rotating stretching sheet.

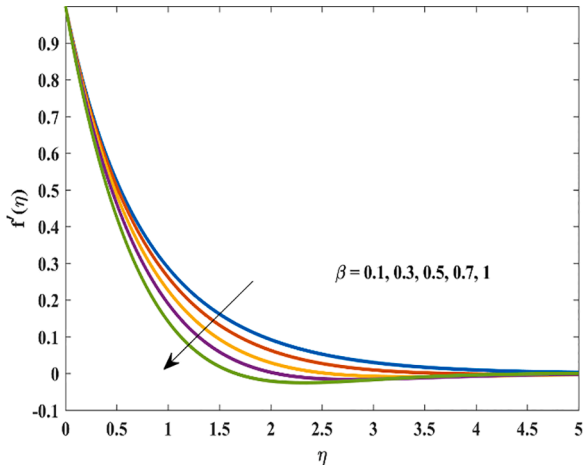

Fig. 2. Effect of βon the dimensionless velocity$f^{'}$

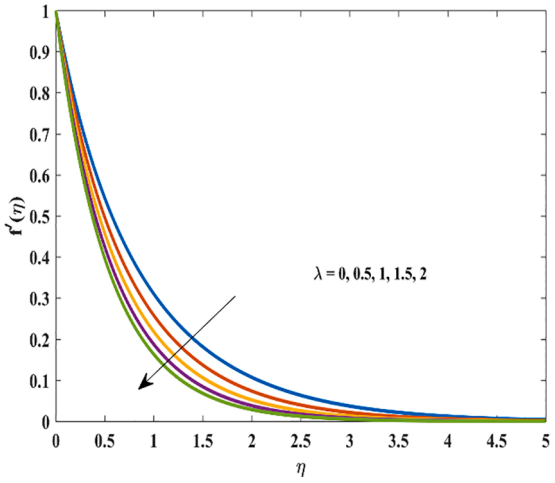

Fig. 3. Influence of λ on the velocity field$f^{'}$

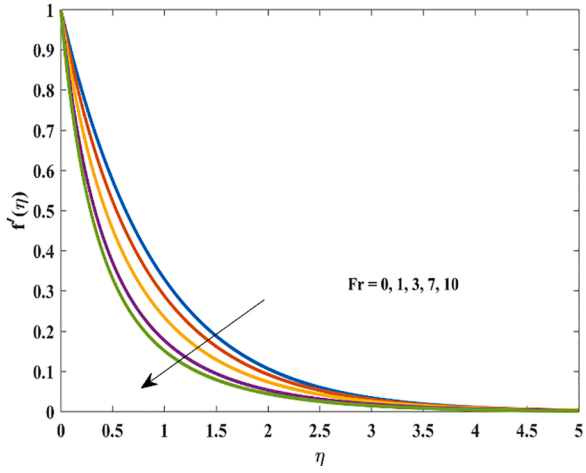

Fig. 4. Behavior of $f^{'}$ for different values of Fr

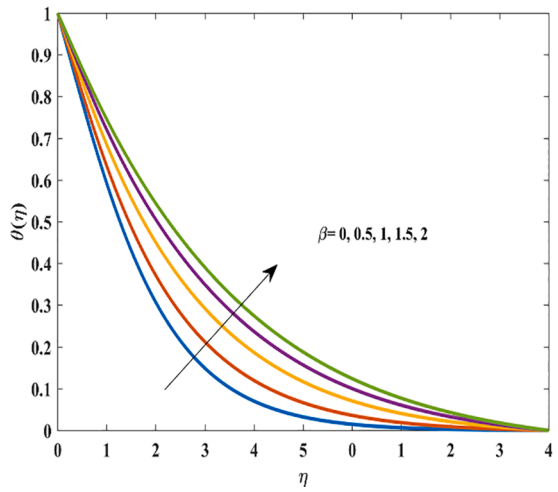

Fig. 5. Impact of parameter β on temperatureθ

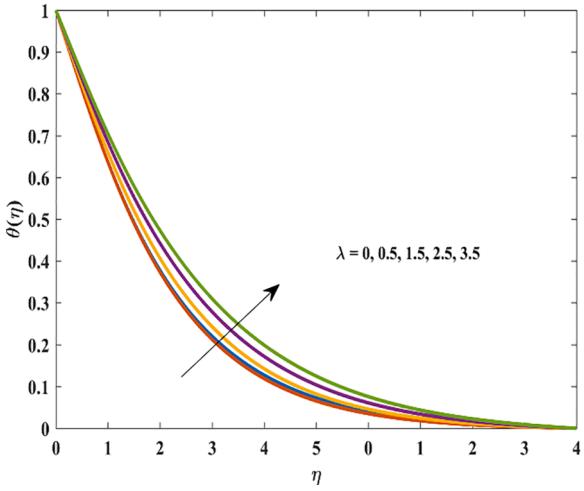

Fig. 6. The impact of porosity number λ on θ

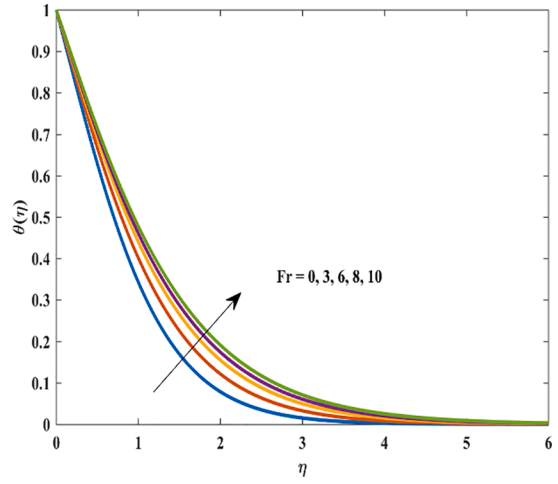

Fig. 7. Graph of θ for different values of *Fr*

decreases. It is apparent from Fig. 17 boosting thickness is reduced by Sc. For larger Sc mass diffusivity rate decreases. It is compelled to decreases in$\varphi(\eta)$. Fig. 18 presents concentration for thermophoresis number$\varphi(\eta)$. Clearly for larger N_t more concentration $\varphi(\eta)$ and layer thickness. Fig. 19 exhibits that concentration $\varphi(\eta)$ reduces forN_b. In Fig. 20 increment the worth of peclet number Pe causes increases in the microorganism diffusivity, hence $\chi(\eta)$ is the microorganisms concentration function which decreases. Fig. 21 shows the behavior of L_b causes decline in diffusivity of the microorganism's motile density. Fig. 4 and 22

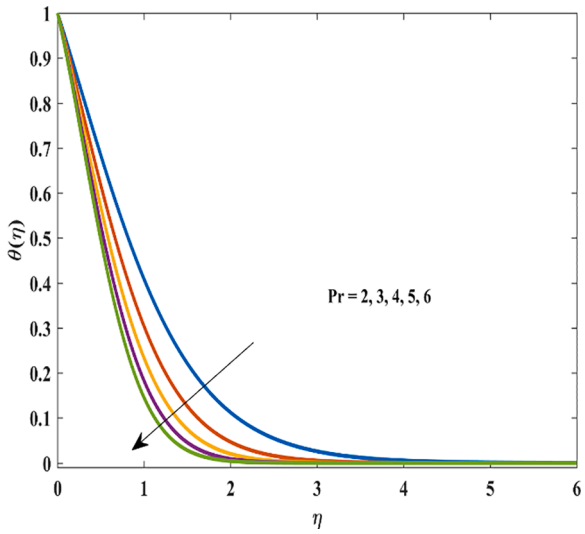

Fig. 8. Curve of θ for various values of *Pr*

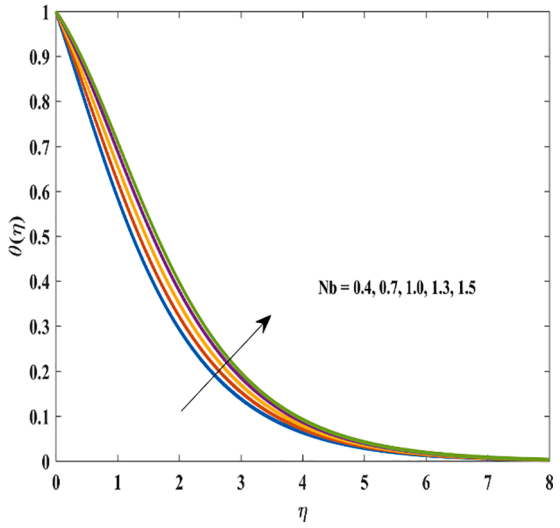

Fig. 9. Behavior of θ for values of N_b

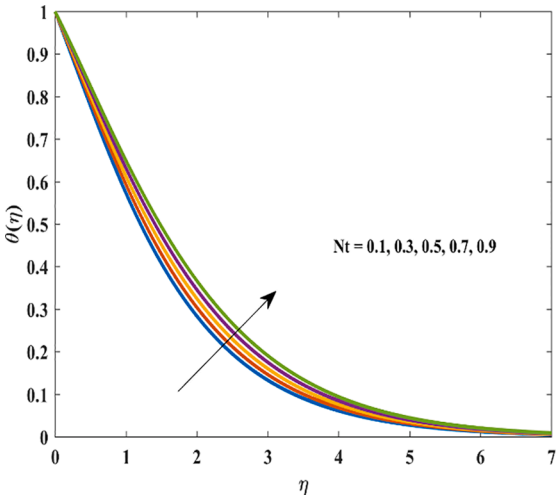

Fig. 10. Influence of parameter $N_t$on the θ

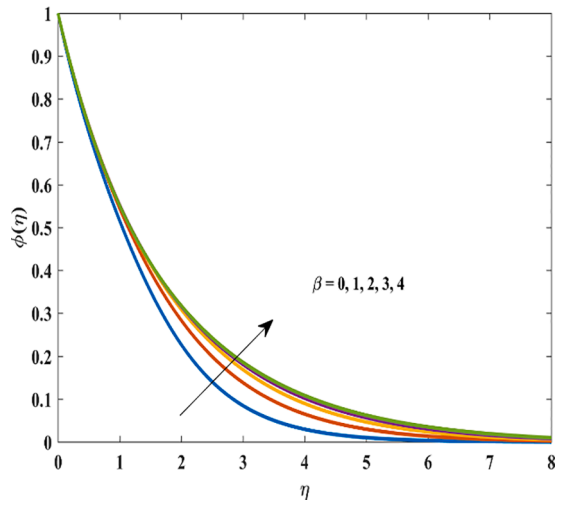

Fig. 11. Effect of φ for distinctive amount of β

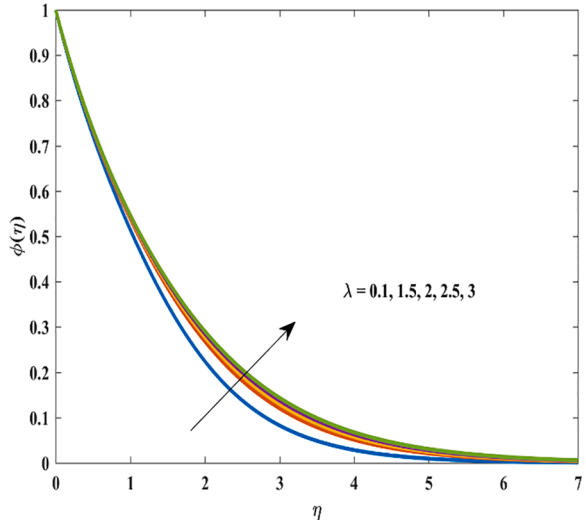

Fig. 12. Influence of $\varphi$for distant amount of λ

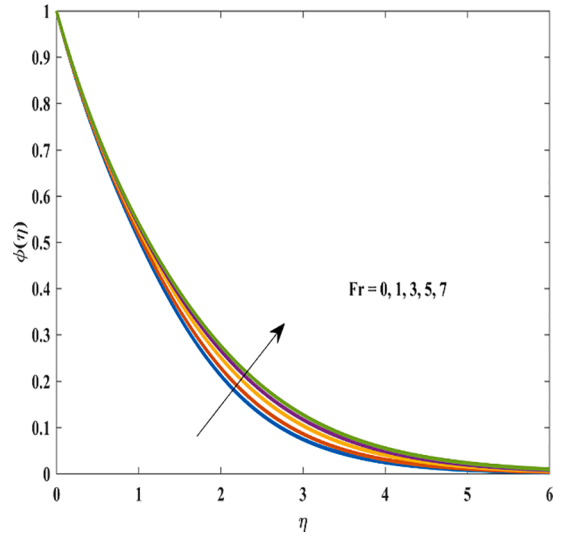

Fig. 13. Impact of parameter Fr on φ

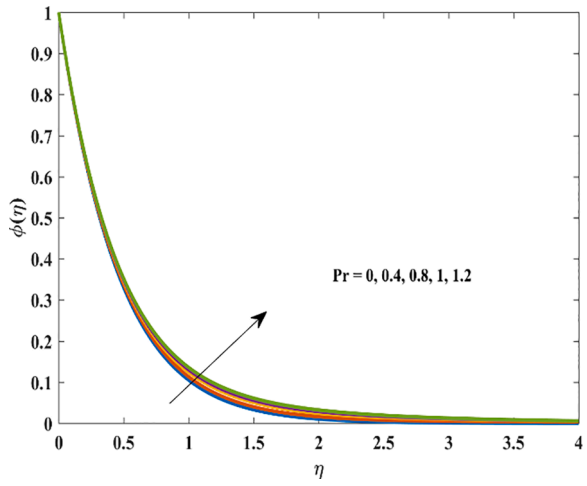

Fig. 14. Behavior of Pr on concentration φ

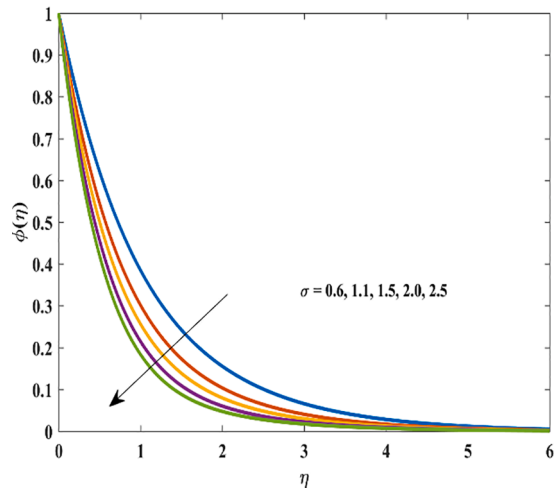

Fig. 17. Impact of φ for distant amount of σ

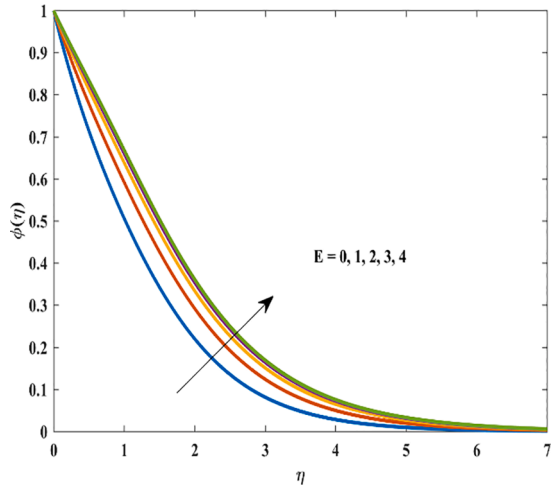

Fig. 15. Curve of φ for various values of E

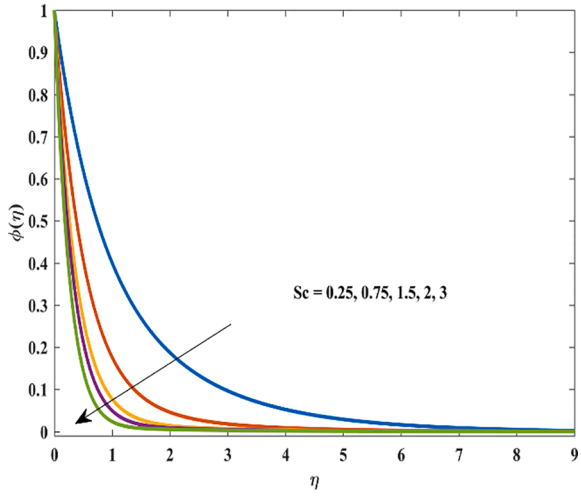

Fig. 18. Effect of φ for distinctive values of Sc

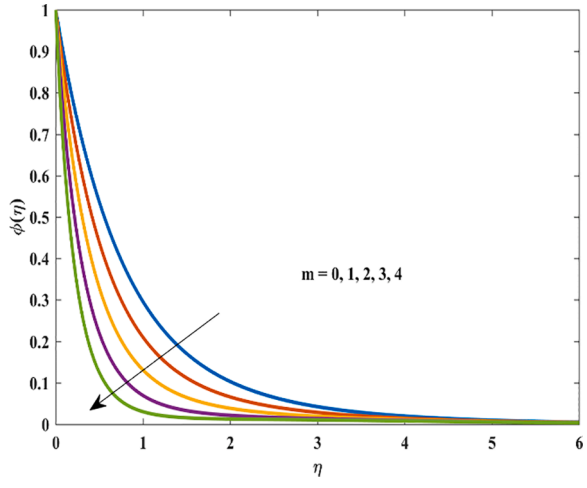

Fig. 16. Influence of φ for various amount of m

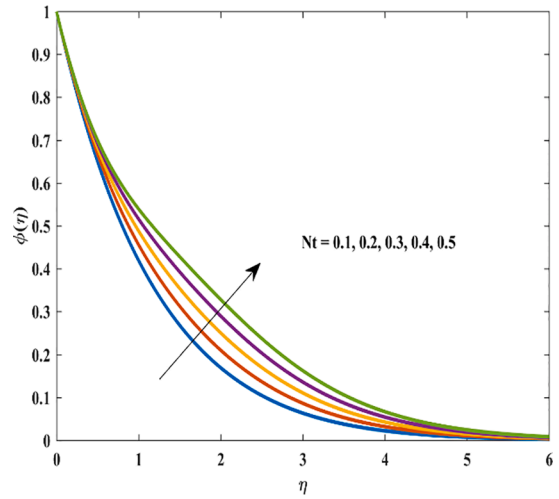

Fig. 19. Impact N_t on concentration φ

5. Conclusion

Heat transfer and magnetohydrodynamic boundary layer flow for nano fluids over a extending sheet has been investigated numerically. Biocnvection of microorganisms is discuss. The effects of the physically parameters of the study have been observed on velocity, microorganisms, concentration and temperature distribution. The main finding of

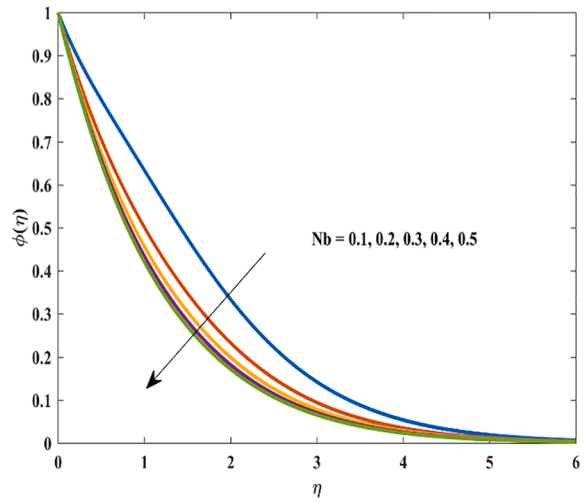

Fig. 20. Effect of Brownion motion number $N_b$on φ

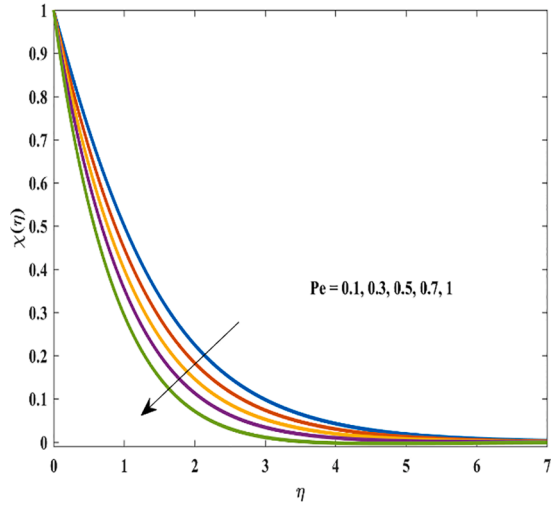

Fig. 21. Impact of bio Lewis number Pe on χ

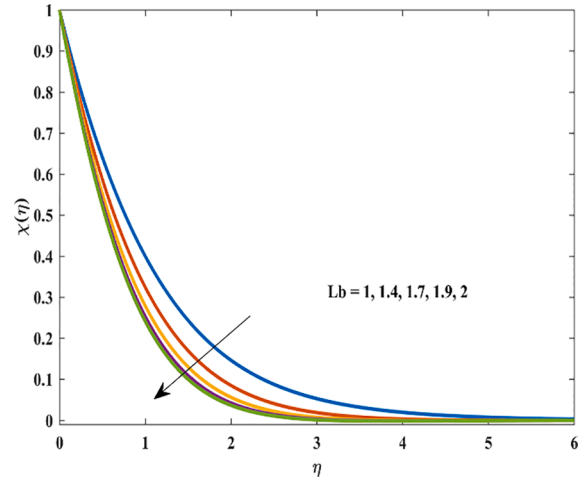

Fig. 22. Influence of Lewis number Lb on χ

this research work is given below as:

- An accumulation in porosity number λ grounds deterioration in velocity $f'(\eta)$ though there is reverse behavior for $\theta(\eta)$ and $\varphi(\eta)$ fields.
- Fluid temperature and nano particle concentration φshow rising behavior withβ.
- There is a decreasing impact of Pr on temperature and concentration.
- Concentration φ is reducing function of constant of reaction rateσ.
- Skin friction coefficient exceeds for λ andβ .
- Temperature gradient $-\theta'(0)$ is decreased against λ andβ.
- The function $\theta(\eta)$ and $\varphi(\eta)$ showed increasing response to thermophoresis parameter N_t
- The N_b parameter of Brownian motion noticeable growing impact on $\varphi(\eta)$ concentration of nano particles but decreasing N_b for $\theta(\eta)$ temperature.
- The concentration of microorganism is improved for greater peclet number Pe but it lessens with growth in bioconvection Lewis numberL_b.

This work could be a sign motivation for the more extension such as Maxwell nanofluid, Hybrid nanofluid, Oldroyd-B and some other sort of nanofluids under different boundary conditions and different physical parameters.

Funding

Not applicable.

Availability of data and materials

Not applicable.

Authors' contributions

Both authors have equal contributions.

Declaration of competing interest

The authors declare that they have no known competing financial interests or personal relationships that could have appeared to influence the work reported in this paper.

Acknowledgement

Not applicable.

References

Choi, S.U., Eastman, J.A., 1995. Enhancing thermal conductivity of fluids with nanoparticles (No. ANL/MSD/CP-84938; CONF-951135-29). Argonne National Lab., IL (United States). ASME 66, 99–105.

Kasaragadda, S., Alarifi, I.M., Rahimi-Gorji, M., Asmatulu, R., 2020. Investigating the effects of surface superhydrophobicity on moisture ingression of nanofiber-reinforced bio-composite structures. Microsystem Technologies 26 (2), 447–459.

Kumar, R.N., Gowda, R.P., Abusorrah, A.M., Mahrous, Y.M., Abu-Hamdeh, N.H., Issakhov, A., Prasannakumara, B.C., 2021. Impact of magnetic dipole on ferromagnetic hybrid nanofluid flow over a stretching cylinder. Physica Scripta 96 (4), 045215.

Khan, W.A., Makinde, O.D., Khan, Z.H., 2014. MHD boundary layer flow of a nanofluid containing gyrotactic microorganisms past a vertical plate with Navier slip. International journal of heat and mass transfer 74, 285–291.

Ali, B., Yu, X., Sadiq, M.T., Rehman, A.U., Ali, L., 2020. A finite element simulation of the active and passive controls of the MHD effect on an axisymmetric nanofluid flow with thermo-diffusion over a radially stretched sheet. Processes 8 (2), 1–19.

Hayat, T., Qayyum, S., Alsaedi, A., Shafiq, A., 2016. Inclined magnetic field and heat source/sink aspects in flow of nanofluid with nonlinear thermal radiation. International Journal of Heat and Mass Transfer 103, 99–107.

Buongiorno, J., 2006. Convective transport in nanofluids. ASME J. Heat transfer. 128, 240–250.

Sreedevi, P., Reddy, P.S., Chamkha, A., 2020. Heat and mass transfer analysis of unsteady hybrid nanofluid flow over a stretching sheet with thermal radiation. SN Applied Sciences 2 (7), 1–15.
Kishan, N., Deepa, G., 2012. Viscous dissipation effects on stagnation point flow and heat transfer of a micropolar nanofluid with uniform suction or blowing. Adv. Appl. Sci. 3, 430–439.
Alim, M.A., Alam, M.M., Mamun, A.A., Hossain, B., 2008. Combined effect nanofluid flow of viscous dissipation and Joule heating on the coupling of conduction and free convection along a vertical flat plate. Int. Commun. Heat Mass Transfer. 35, 338–346.
Hayat, Tasawar, Qayyum, Sumaira, Alsaedi, Ahmed, Ahmad, Bashir, 2020. Entropy generation minimization: Darcy-Forchheimer nanofluid flow due to curvd stretching sheet with partial slip 111, 104445.
Khan, W.A., Pop, I., 2010. Boundary-layer flow of a nanofluid past a stretching sheet. International journal of heat and mass transfer 53 (11-12), 2477–2483.
Wang, P., Zhu, X., Li, Y., 2020. Analysis of Flow and Wear Characteristics of. Processes 8, 1512.
Kotresh, M.J., Ramesh, G.K., Shashikala, V.K.R., Prasannakumara, B.C., 2021. Assessment of Arrhenius activation energy in stretched flow of nanofluid over a rotating disc. Heat Transfer 50 (3), 2807–2828.
Krishna, M Veera, Chamkha, Ali J, 2020. Hall and ion slip effects on MHD rotating flow of elastico-viscous fluid through porous medium. Journal, International Communications in Heat and Mass Transfer 13, 104494.
Kanta Mondal, S., Pal, D., 2020. Gyrotactic mixed bioconvection flow of a nanofluid over a stretching wedge embedded in a porous media in the presence of binary chemical reaction and activation energy. International Journal of Ambient Energy 1–11.
Sk, Md Tausif, Das, Kalidas, Kundu, Prabir Kumar, 2016. Multiple slip effects on bioconvection of nanofluid flow containing gyrotactic microorganisms and nanoparticles. Journal of Molecular Liquids 220, 518–526.
Kuznetsov, A.V., Avramenko, A.A., 2004. Efect of small particles on the stability of bioconvection in a suspension of gyrotactic microorganisms in a layer of fnite depth. Int. Communi, Heat Mass Transf 31, 1–10.
Zeeshan, A., Ali, Z., Gorji, M.R., Hussain, F., Nadeem, S., 2020. Flow analysis of biconvective heat and mass transfer of two-dimensional couple stress fluid over a paraboloid of revolution. International Journal of Modern Physics B 34 (11), 2050110.
Makinde, O.D., Animasaun, I.L., 2016. Bioconvection in MHD nanofluid flow with nonlinear thermal radiation and quartic autocatalysis chemical reaction past an upper surface of a paraboloid of revolution. International Journal of Thermal Sciences 109, 159–171.
Makinde, O.D., Animasaun, I.L., 2016. Thermophoresis and Brownian motion effects on MHD bioconvection of nanofluid with nonlinear thermal radiation and quartic chemical reaction past an upper horizontal surface of a paraboloid of revolution. Journal of Molecular liquids 221, 733–743.
Avinash, K., Sandeep, N., Makinde, O.D., Animasaun, I.L., 2017. Aligned magnetic field effect on radiative bioconvection flow past a vertical plate with thermophoresis and Brownian motion. Defect and Diffusion Forum (Vol. 377, pp. 127-140). Trans Tech Publications Ltd.
Shafiq, A., Sindhu, T.N., Khalique, C.M., 2020. Numerical investigation and sensitivity analysis on bioconvective tangent hyperbolic nanofluid flow towards stretching surface by response surface methodology. Alexandria Engineering Journal 59 (6), 4533–4548.
Shafiq, A., Lone, S.A., Sindhu, T.N., Al-Mdallal, Q.M., Rasool, G., 2021. Statistical modeling for bioconvective tangent hyperbolic nanofluid towards stretching surface with zero mass flux condition. Scientific Reports 11 (1), 1–11.
Ali, B., Nie, Y., Hussain, S., Manan, A., Sadiq, M.T., 2020. Unsteady Magneto-hydrodynamic Transport of Rotating Maxwell Nanofluid Flow on a Stretching Sheet With Cattaneo–Christov Double Diffusion and Activation Energy. Thermal Science and Engineering Progress 8 (2), 1–19.
Ali, Bagh, Pattnaik, PK, Naqvi, Rizwan Ali, Waqas, Hassan, Hussain, Sajjad, 2021. Brownian motion and thermophoresis effects on bioconvection of rotating Maxwell nanofluid over a Riga plate with Arrhenius activation energy and Cattaneo-Christov heat flux theory. Journal, Thermal Science and Engineering Progress 23, 100863.
Gowda, R.P., Al-Mubaddel, F.S., Kumar, R.N., Prasannakumara, B.C., Issakhov, A., Rahimi-Gorji, M., Al-Turki, Y.A., 2021. Computational modelling of nanofluid flow over a curved stretching sheet using Koo–Kleinstreuer and Li (KKL) correlation and modified Fourier heat flux model. Chaos, Solitons & Fractals 145, 110774.
Balla, C.S., Alluguvelli, R., Naikoti, K., Makinde, O.D., 2020. Effect of chemical reaction on bioconvective flow in oxytactic microorganisms suspended porous cavity. Journal of Applied and Computational Mechanics 6 (3), 653–664.
Varun Kumar, R.S., Alhadhrami, A., Punith Gowda, R.J., Naveen Kumar, R., Prasannakumara, B.C, 2021. Exploration of Arrhenius activation energy on hybrid nanofluid flow over a curved stretchable surface. ZAMM-Journal of Applied Mathematics and Mechanics/Zeitschrift für Angewandte Mathematik und Mechanik, e202100035.
Ramesh, G.K., Madhukesh, J.K., Prasannakumara, B.C., Roopa, G.S., 2021. Significance of aluminium alloys particle flow through a parallel-plates with activation energy and chemical reaction. Journal of Thermal Analysis and Calorimetry 1–11.
Shi, Q.H., Hamid, A., Khan, M.I., Kumar, R.N., Gowda, R.J., Prasannakumara, B.C., Chung, J.D., 2021. Numerical study of bio-convection flow of magneto-cross nanofluid containing gyrotactic microorganisms with activation energy. Scientific Reports 11 (1), 1–15.
Madhukesh, J.K., Ramesh, G.K., Kumar, R.V., Prasannakumara, B.C., Alaoui, M.K., 2021. Computational study of chemical reaction and activation energy on the flow of Fe3O4-Go/water over a moving thin needle: Theoretical aspects. Computational and Theoretical Chemistry, 113306.
Rashid, Sadia, Hayat, Tasawar, Qayyum, Sumaira, Ayub, Muhammad, Alsaedi, Ahmed, 2018. Three dimensional rotating Darcy–Forchheimer flow with activation energy. International Journal of Numerical Methods for Heat & Fluid Flow 29 (3), 935–948.
Kuznetsov, A.V., 2011. Bio-thermal convection induced by two different species of microorganisms. International Communications in Heat and Mass Transfer 38 (5), 548–553.
Ali, L., Wang, Y., Ali, B., Liu, X., Din, A., Al Mdallal, Q., 2021. The function of nanoparticle's diameter and Darcy-Forchheimer flow over a cylinder with effect of magnetic field and thermal radiation. Case Studies in Thermal Engineering 28, 101392.
Zhao, B.Q., Pantokratoras, A., Fang, T.G., Liao, S.J., 2010. Flow of a weakly conducting fluid in a channel filled with a Darcy–Brinkman–Forchheimer porous medium. Transport in porous media 85 (1), 131–142.
Ali, B., Naqvi, R.A., Hussain, D., Aldossary, O.M., Hussain, S., 2020. Magnetic Rotating Flow of a Hybrid Nano-Materials Ag-MoS2 and Go-MoS2 in C2H6O2-H2O Hybrid Base Fluid over an Extending Surface Involving Activation Energy. FE Simulation. Mathematics 8 (10), 1730.